The Effects of a Storm Surge Event on Salt Intrusion
Insights From the Rhine-Meuse Delta

Gerritsma, A.; Verlaan, M.; Geraeds, M.; Huismans, Y.; Pietrzak, J.D.

DOI
10.1029/2024JC021520

Publication date
2025

Document Version
Final published version

Published in
Journal Of Geophysical Research-Oceans

JGR Oceans

RESEARCH ARTICLE
10.1029/2024JC021520

The Effects of a Storm Surge Event on Salt Intrusion: Insights From the Rhine-Meuse Delta

Avelon Gerritsma[1], Martin Verlaan[1,2], Marlein Geraeds[3], Ymkje Huismans[2,3], and Julie Pietrzak[3]

[1]Department of Applied Mathematics, Delft University of Technology, Delft, The Netherlands, [2]Deltares, Delft, The Netherlands, [3]Department of Hydraulic Engineering, Delft University of Technology, Delft, The Netherlands

Key Points:

- A 3-D model was developed that successfully reproduces salt transport in a complex delta
- Salt can remain in semi-enclosed regions with low flow velocities after a storm surge, leading to prolonged elevated salinity levels
- While salt intrusion during a storm is driven by a barotropic pressure gradient, stratification plays an important role in retaining salt

Correspondence to:
A. Gerritsma,
a.gerritsma@tudelft.nl

Citation:
Gerritsma, A., Verlaan, M., Geraeds, M., Huismans, Y., & Pietrzak, J. (2025). The effects of a storm surge event on salt intrusion: Insights from the Rhine-Meuse Delta. *Journal of Geophysical Research: Oceans*, *130*, e2024JC021520. https://doi.org/10.1029/2024JC021520

Received 28 JUN 2024
Accepted 18 MAR 2025

Author Contributions:
Conceptualization: Avelon Gerritsma, Martin Verlaan, Julie Pietrzak
Formal analysis: Avelon Gerritsma
Investigation: Avelon Gerritsma
Methodology: Avelon Gerritsma, Martin Verlaan, Marlein Geraeds, Ymkje Huismans, Julie Pietrzak
Supervision: Martin Verlaan, Julie Pietrzak
Validation: Avelon Gerritsma
Visualization: Avelon Gerritsma, Marlein Geraeds
Writing – original draft: Avelon Gerritsma
Writing – review & editing: Avelon Gerritsma, Martin Verlaan, Marlein Geraeds, Ymkje Huismans, Julie Pietrzak

Abstract The Rhine-Meuse Delta is a low-lying delta in the Netherlands that is subject to both salt intrusion events and storm surges. Typically, storm surges only temporarily cause increased salt intrusion and do not cause severe problems for freshwater availability. However, during the storm surge of December 2013, salt reached the closed southern branch of the delta and higher salinities were observed for weeks after the storm surge. The purpose of this study is to examine the mechanisms controlling salt intrusion in the Rhine-Meuse Delta during and after a severe storm surge event. A three-dimensional hydrodynamic model (Delft3D-FM) of the Rhine-Meuse Delta was developed that successfully reproduces salt intrusion for both normal and storm surge conditions. During the storm, high water levels in the northern branch caused a salt flux toward the southern branch. The southern branch of the Rhine-Meuse Delta is closed off by an estuarine dam, consequently salt was retained landward of the dam. Local stratification in the southern branch caused salt to remain in the deeper parts, limiting the effectiveness of flushing after the storm surge. In the post-storm period, salt was gradually released from the southern branch, raising salinity levels in an adjacent channel. The river discharge was only just below the yearly average, showing prolonged salt intrusion can also occur outside of dry periods.

Plain Language Summary Salt intrusion, the process of seawater intruding freshwater systems, is mainly governed by variations in discharge, tide, and storm surges. Storm surges typically cause increased salt intrusion for short periods of time and do not cause severe problems for freshwater availability. However, there have been a few occurrences in the Rhine-Meuse Delta where higher salinities were observed for weeks after a storm surge event. To understand and predict salt intrusion for both normal and storm conditions, we developed a three-dimensional model of the Rhine-Meuse Delta, with which we modeled an exceptional storm surge event in December 2013. During the storm surge, a mass of salt water entered the northern branch of the delta and flowed toward the southern branch. Since the southern branch is closed off by an estuarine dam, the salt that entered during the storm was retained landward of the dam. In the weeks after the storm surge, salt was gradually released from the southern branch, raising salinity levels in an adjacent channel. This shows that the effects of storm surges on salt intrusion can last longer when salt is retained in the system.

1. Introduction

Severe salt intrusion events pose a threat to the drinking water supply, ecological health, and economic interests in estuaries all around the world (Cook et al., 2023; Eslami et al., 2021; Hu et al., 2023; Tsai et al., 2024; J. Zhu et al., 2020). The estuarine salinity distribution is influenced by the balance between seaward advection of salt by the freshwater discharge and landward salt transport by estuarine circulation and tidal dispersion (Fischer, 1972; Hansen & Rattray, 1965; Lerczak et al., 2006). Severe salt intrusion is often related to droughts, when low frequency subtidal transport and wind-driven transport drive the salt front further upstream (Banas et al., 2004; Bowen, 2003; Lerczak et al., 2009). However, storm surges can also drastically increase the salt intrusion length (Cook et al., 2023). Few studies have investigated the dynamics of a storm surge event on salt intrusion in detail, and even less in a delta with multiple side branches and human modifications. In this paper, we analyze the effects of storm surge on salt intrusion for the Rhine-Meuse Delta using unique observations and a numerical model.

Storm surge is caused by surface wind stress and atmospheric pressure perturbations, commonly associated with low pressure systems (Flather, 2001). The elevated water levels at the coast drive a barotropic landward flow of salt water, resulting in higher salinities in the estuary. Eslami et al. (2021) found that up to 20% of the subtidal salinity variation in the Mekong Delta could be explained by storm surges. During dry season, the salt intrusion length (SIL) was more sensitive to surge height than typical variations in river discharge. An observational study

in the Delaware Bay showed that the sea surface height, influenced by tropical cyclones, was the main driver for the landward advective salt flux (Aristizabal & Chant, 2015). This landward advective salt flux often dominated over the seaward flux associated with river discharge, resulting in a net landward flux that persisted for several days. Moreover, a numerical model study for the same estuary found individual storms could move the salt front 13–16 km landwards (Cook et al., 2023).

While salt intrusion during droughts can last for months, the excessive salt concentrations during storms typically lasts for a few days. Even for the extreme case of a low pressure system, during the passing of a tropical cyclone, studies report only short-term effects on the estuarine salinity (Cho et al., 2012; L. Li et al., 2022). L. Li et al. (2022) studied the effects of the passing of a tropical cyclone on salt intrusion in the Changjiang estuary (also known as Yangtze estuary). They found that the landward salt transport lasted for 1.7 days, then shifted seaward approximately 1 day after the storm passed. The salt was flushed out of the system in 3.5 days. After a storm surge, salt is generally flushed out of the system, unless a substantial amount of salt water stays behind in sheltered zones. Such long-term effects of storm surges have not yet been reported in scientific literature, but have been observed in the Rhine-Meuse Delta. An illustrative example was the Sinterklaasstorm that occurred on December 5th and 6th 2013, when salinities exceeding the Dutch norm for freshwater intake (0.27 psu) were observed for weeks (De Vries, 2014).

The geometry of the Rhine-Meuse Delta and human modifications play an important role in the system's response to surges. The Rhine-Meuse Delta has two main branches that discharge into the North Sea. The northern branch, the Rotterdam Waterway, has an open connection with the North Sea and is the main outlet of the River Rhine. The southern branch, the Haringvliet, is closed off by an estuarine dam (the Haringvlietdam), built in 1970 to protect the South-West of the Netherlands against flooding. The estuarine dam incorporates floodgates to control water levels and freshwater discharge. When the floodgates are closed, the southern branch is closed off and is therefore predominantly fresh. However, when during a storm surge, salt water reaches the southern branch via the northern inlet, the closed branch can also retain the salt water in the system.

Estuaries worldwide are increasingly managed, with estuarine dams and barriers being considered to protect against storm surges (Ralston, 2022). These coastal structures can greatly alter the hydrodynamics inland, including tidal amplification, reduced tidal currents, and changes in stratification (Figueroa et al., 2022; Orton et al., 2023). In the Netherlands, there are three estuarine dams closing Lake IJssel, Lake Grevelingen, and the Haringvliet (Tönis et al., 2002). These measures were designed for water safety, yet is important to understand how the changed hydrodynamics can affect the water quality.

Salt intrusion into the Haringvliet via the northern inlet is currently predicted by a simple tool, based on the water level difference between the northern and southern branch (Huismans et al., 2019). A three-dimensional hydrodynamic model could support optimal water management and provide insights into the mechanisms controlling salt intrusion during a severe storm surge event. For example, to understand the prolonged elevated salinities levels after the 2013 storm surge event. Furthermore, future sea level rise can potentially increase the impact of storm surges on salt intrusion. This highlights the importance of fundamental understanding and advanced 3D modeling of salt intrusion in complex deltas during storm surges.

The aim of this study is to improve our understanding of the physical processes governing salt intrusion during and after storm surges and develop a numerical model to forecast them. After model development and validation, we simulated the 2013 storm surge event. The paper is organized as follows. Section 2 presents the study area and the hydrodynamic model. Results of the model validation and the 2013 storm event are presented in Section 3. Section 4 discusses our results in comparison with previous work and implications of our findings. Final conclusions are made in Section 5.

2. Methods

2.1. Study Area

The Rhine-Meuse Delta in the Netherlands is fed by the rivers Rhine and Meuse, which are controlled by weirs in the upstream part. Shortly after crossing the Dutch-German border at Lobith, the Rhine splits into the Waal and the Nederrijn (called Lek further downstream), which are also controlled by weirs and sluices. Figure 1 shows the position of the Rhine-Meuse Delta and names of the river branches. The Meuse (Maas) enters the Netherlands in the south and bends seawards at Nijmegen to continue running parallel to the Waal. The largest part of the total

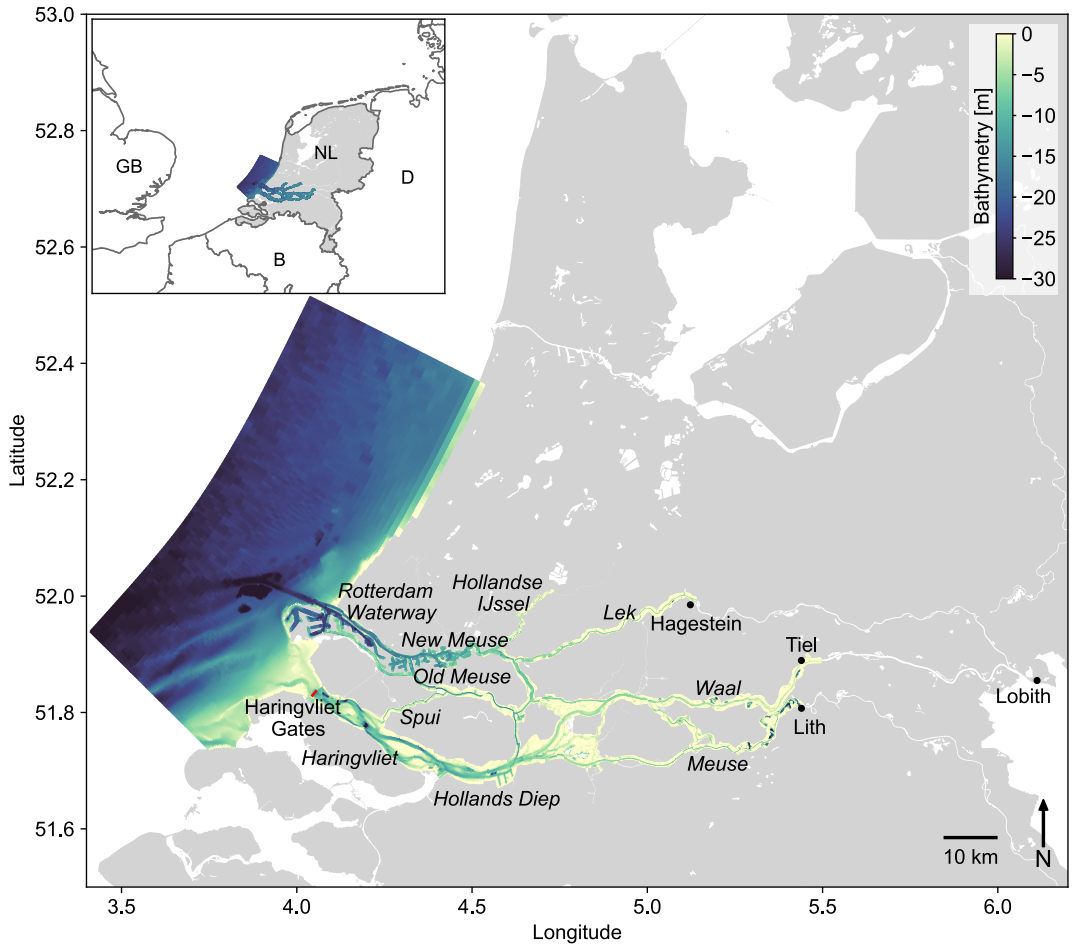

Figure 1. Map showing the location of the Rhine-Meuse Delta and the model bathymetry. Names of the river branches in italic.

discharge entering the Rhine-Meuse Estuary comes from the Waal (70%). The Lek and Meuse have a similar discharge magnitude, 16% and 14% of the total discharge, respectively (Cox et al., 2021). In the lower part of the delta, the Waal, Lek, and Maas split into a complex network of branches interconnected by various channels. Finally, two branches end up in the North Sea, the Rotterdam Waterway and the Haringvliet.

The Rhine-Meuse Delta is a mesotidal salt wedge estuary (de Nijs et al., 2011). On average, the salt wedge reaches until the bifurcation point of the Rotterdam Waterway and Old Meuse. In dry summers, the salt reaches farther into the river system, up to the River Lek and Hollandse IJssel. The Old Meuse and Spui are well-mixed or weakly stratified for normal conditions. The Haringvliet is stratified with a pycnocline close to the bed (Kranenburg et al., 2023).

The floodgates in the Haringvlietdam (red line in Figure 1) remain closed during flood tide, allowing only regulated outflow during ebb tide based on the river discharge. During periods of low river discharge, the gates remain closed during ebb, directing the majority of water through the northern branch (Rotterdam Waterway) to limit salt intrusion. The tide enters and leaves the southern branch (Haringvliet) via the northern branch. One can define two phases in the tidal cycle: (a) when the water level is higher in the northern branch and flow is directed toward the southern branch and (b) when the water level is higher in the southern branch and the flow is directed toward the northern branch. The duration of the first phase is generally shorter and the water level difference is smaller, resulting in a net flow toward the northern branch, limiting salt intrusion (Huismans, 2016). During a storm surge, elevated water levels in the Rotterdam Waterway extend the duration of the first phase and increase the water level difference, whereas the second phase is shorter and the gradient is reduced. As a result, a net flux of salt water enters the Haringvliet via the backdoor, also known as “backwards salinization” (Huismans, 2016).

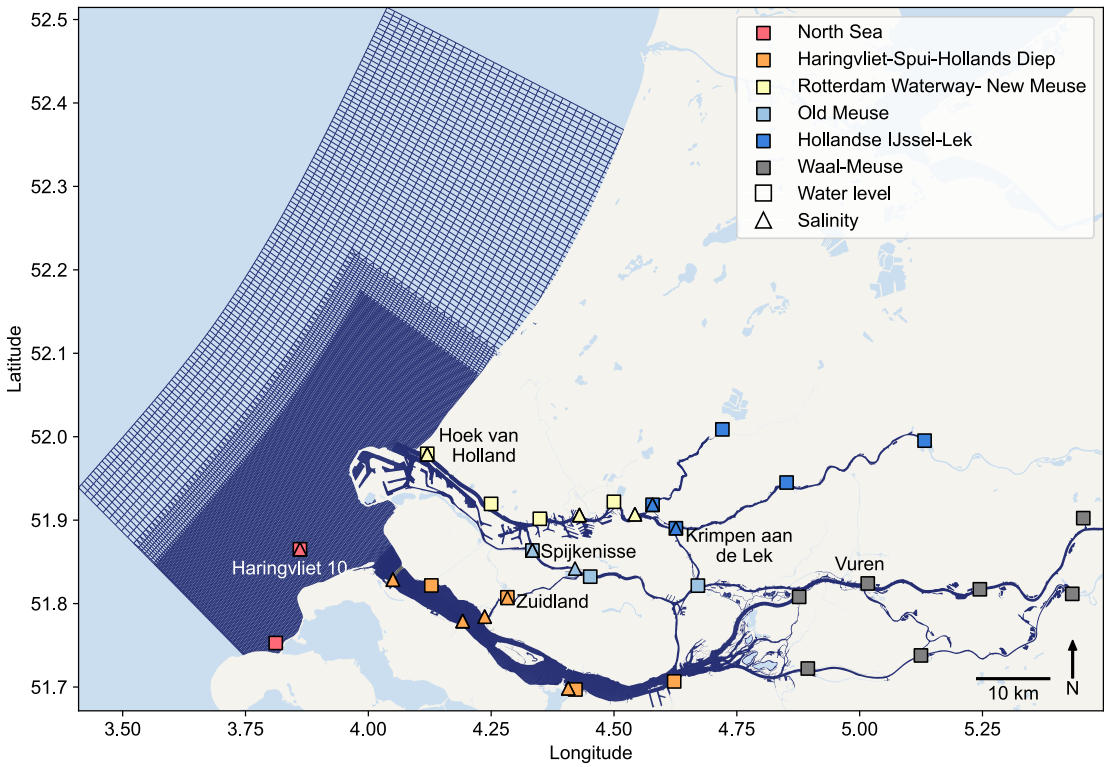

Figure 2. Rhine-Meuse Delta model grid. Triangles and squares indicate salinity and water level observation locations, respectively. Colors show the different regions used for model validation.

2.2. Hydrodynamic Model

The RMD model is developed using Delft3D-Flexible Mesh (Delft3D-FM), which solves the nonlinear shallow-water equations for curvilinear and unstructured grids (Kernkamp et al., 2011). Figure 2 displays the model domain and grid. The model stretches 35 km seawards from the Dutch coast. Cell sizes range from 600 × 1,200 m at the sea boundary and refine toward the coast with cells of 170 × 290 m. The river branches are at least 8 cells wide (20 m), and cells are 60–100 m long depending on the river branch.

In the vertical, the model has z-layers close to the bed and 9 σ-layers at the surface. Above −15 m, the z-layer thickness remains constant at 75 cm, below this depth, the thickness increases downwards with a factor of 1.1. The σ-layer thickness varies between 40 and 75 cm through time depending on the water level. Model settings for vertical layering and transport of matter are based on earlier work (van der Kaaij & Chavarrias, 2020) and listed in Table 1. The horizontal diffusivity consists of three parts: a constant background diffusivity, a varying sub-grid scale turbulence using Smagorisky, and a varying part determined by the k-ϵ turbulence model. The vertical diffusion consists of a constant background diffusivity and a varying part determined by the k-ϵ turbulence model.

Table 1
Model Settings

Parameter	Value
Code version	2023.03
Vertical layer type	z-σ
Max nr. of vertical layers	36
Horizontal viscosity/diffusivity	$1 \cdot 10^{-2} m^2/s$
Vertical viscosity/diffusivity	$5 \cdot 10^{-5} m^2/s$
Smagorinsky factor	0.10
Turbulence closure scheme	k-ϵ

The bathymetry of the RMD model is visualized in Figure 1. The maximum depth at sea reaches 35 m, and at Hoek van Holland the estuary is 15 m deep. A spatially varying bed roughness is applied, with a Manning formulation in the tide dominated region and a simplified version of the van Rijn formulation (van Rijn, 1984) in the discharge-dominated river branches. In addition, vegetation is represented in the roughness to account for its flow resistance. The RMD model includes the following main structures: the Haringvlietdam, the Maeslant- and Hartel barrier, and the Volkerakdam. Lastly, other relevant features such as dikes and groynes are represented in the model by fixed weirs.

2.3. Model Forcing

At the sea boundary, we imposed a water level time series obtained by nesting the model in the Dutch Continental Shelf Model (DCSM) with Kalman Filter correcting water levels with observations (Zijl et al., 2015). The 3D boundary conditions for salinity and temperature were obtained using a 3D version of the DCSM model. The river discharges at Hagestein, Tiel, and Lith (Megen) are made publicly available by *Rijkswaterstaat* (https://waterinfo.rws.nl). A 2 hr smoothing filter was applied to the 10 min river discharges to remove high-frequent noise. Next to the river discharge time series at the model boundaries, laterals (canals, small streams) were included in the model to represent inflow or outflow of water. The river background salinity was estimated based on the chloride concentration at Eijsden for the Maas and at Lobith for the Lek and Waal, accounting for the time lag between these upstream stations and the model boundary. The meteorological forcings, air pressure and wind speed, are provided by the *KNMI* from the High Resolution Limited Area Model (HiRLAM).

2.4. Computational Performance

The RMD model achieves a performance of ∼144 times faster than real time, using 96 cores on the Snellius, the Dutch National supercomputer hosted at SURF (dual socket AMD Genoa 9,654 node with 384 GiB memory). The computation time step was limited based on the Courant criterium and varied between 8 and 15 s.

2.5. Model Validation

The hydrodynamic model was run for the period 1 November 2012–31 December 2013. The model is validated for the year 2013, with two spin-up months in advance. The data during the spin-up are discarded. The water level and salinity observations used to validate our model, with a 10-min frequency, were provided by *Rijkswaterstaat* (https://waterinfo.rws.nl). The model performance for salinity and water levels is evaluated using four metrics. The Root Mean Squared Error (RMSE) and Bias between model (x_i) and observations (z_i):

$$\mathrm{RMSE} = \sqrt{\frac{1}{N}\sum_{i=1}^{N}(x_i - z_i)^2}, \tag{1}$$

$$\mathrm{Bias} = \frac{1}{N}\sum_{i=1}^{N}(x_i - z_i) \tag{2}$$

Furthermore, we calculate sample correlation coefficient

$$\mathrm{r} = \frac{\sum_{i=1}^{N}(x_i - \bar{x})(z_i - \bar{z})}{\sqrt{\sum_{i=1}^{N}(x_i - \bar{x})^2}\sqrt{\sum_{i=1}^{N}(z_i - \bar{z})^2}} \tag{3}$$

and the Model Skill Score (MSS) (Ralston et al., 2010), given by:

$$\text{Model Skill Score} = 1 - \frac{\sum_{i=1}^{N}|x_i - z_i|^2}{\sum_{i=1}^{N}|z_i - \bar{z}|^2}. \tag{4}$$

MSS equals 1 when the model exactly agrees with the observations; an MSS smaller/equal to zero indicates the model provides less/equal predictive skill as the mean of the observations. The mean of the observations for the year 2013 was used as reference for the MSS. The metrics were calculated for six sub-areas with similar model performance and characteristics, the observation stations for water level and salinity for the six regions are visualized in Figure 2. We calculated the mean RMSE, bias, r, and MSS of all stations in these sub-areas.

The water level time series were decomposed into a tidal and practical surge signal for separate evaluation. The tidal signal was extracted from the water level time series using harmonic tidal analysis (via hatyan python package). The practical surge signal was obtained by subtracting the tidal signal from the original time series. Subsequently, the RMSE was calculated for both the tidal $(RMSE_t)$ and practical surge $(RMSE_s)$ signal.

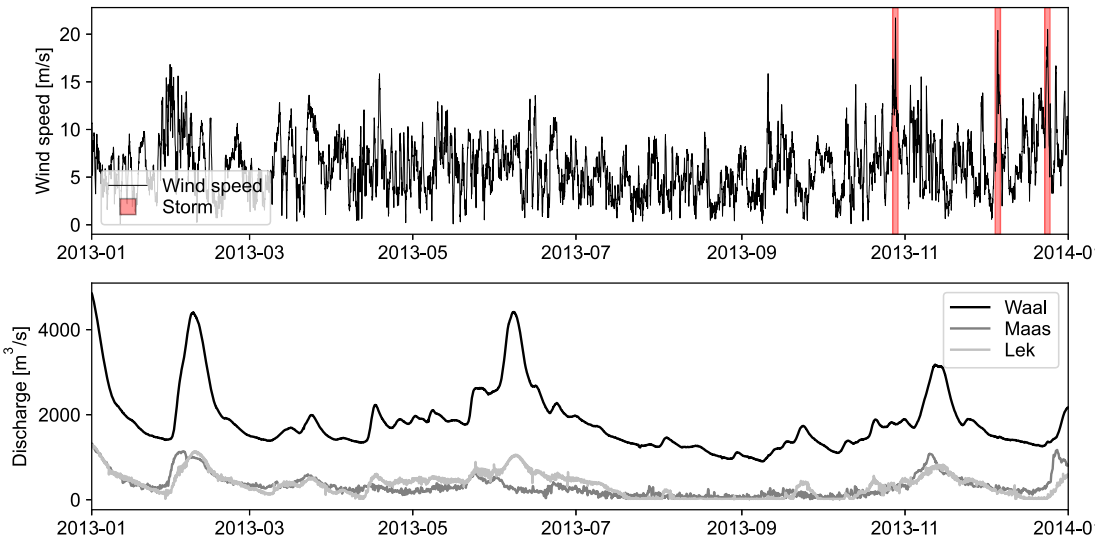

Figure 3. The wind speed at Hoek van Holland and discharge of the rivers Waal, Maas, and Lek for the year 2013. Storm conditions are highlighted in red.

The performance metrics were determined for the whole year and for storm conditions, defined as the days when the hourly mean wind speed is larger than 20 m/s Figure 3 shows the wind speed at Hoek van Holland with storm conditions highlighted in red and the discharge of the rivers Waal, Maas, and Lek in 2013. The second storm on 5-6 December is the Sinterklaasstorm, which is the focus of this study.

3. Results

3.1. Model Validation

The model performance metrics are presented in Table 2, with values for the whole year 2013 in black and for storm conditions in red. First, we will discuss the model performance for water levels. The high Model Skill Scores (0.94–1.00) and correlation coefficients (0.99–1.00) for the validation period for all six sub-areas indicate water levels are simulated well for the whole model domain. The RMSE is calculated for the tidal ($RMSE_t$) and practical surge ($RMSE_s$) signal of the water level time series (described in Section 2.5). The practical surge shows a larger RMSE during storm conditions ($RMSE_s$), especially on the North Sea. Nevertheless, the high MSS and correlation coefficient indicate the model performance is still good for storm conditions.

Table 2
Model Performance Metrics for the Six Sub-Areas

	North sea	Haringvliet-Spui-Hollands Diep	Rotterdam Waterway-New meuse	Old meuse	Hollandse IJssel-Lek	Waal-Meuse
Water level [m]						
Bias	0.00/−0.03	−0.03/0.00	0.01/0.01	−0.01/0.00	0.03/0.04	0.00/0.06
RMSEt	0.03/0.03	0.04/0.04	0.03/0.03	0.04/0.03	0.05/0.05	0.04/0.04
RMSEs	0.03/0.10	0.03/0.05	0.03/0.07	0.03/0.05	0.05/0.10	0.05/0.07
r	1.00/1.00	0.99/0.99	1.00/1.00	1.00/1.00	0.99/0.98	0.99/0.99
MSS	1.00/0.99	0.94/0.99	1.00/0.99	0.99/0.99	0.98/0.97	0.98/0.95
Salinity [psu]						
Bias	−1.07/−0.13	−0.08/−0.09	1.86/1.05	0.30/0.53	−0.02/0.02	–
RMSE	2.02/0.72	0.15/0.33	2.93/2.43	0.87/1.49	0.07/0.26	–
r	0.71/0.94	0.85/0.91	0.86/0.90	0.95/0.97	0.76/0.79	–
MSS	−0.02/0.90	0.62/0.57	0.08/0.74	0.80/0.94	−0.69/−0.39	–

Note. Values for validation year in black and values for storm conditions in red. $RMSE_t$ and $RMSE_s$ are the RMSE's for tidal and practical surge signals, respectively.

Next, we will discuss the model for salinity predictions. Note that the bias and RMSE values for salinity are strongly dependent on the location, where more saline locations will generally get higher values. The MSS and correlation coefficients for salinity are lower than for water level. Nevertheless, for storm conditions the model performs surprisingly well with correlation coefficients between 0.79 and 0.94. The largest salinity bias is in the Rotterdam Waterway. The Rotterdam Waterway is strongly stratified, which is challenging to model accurately (M. Li et al., 2005). The performance metrics for the North Sea were calculated for one of the two stations (Haringvliet 10), as the measurements of the other station were unreliable due to biofouling. The background concentration on the Hollandse IJssel and Lek was slightly underestimated by the model, which explains the negative MSS as the average of measurements is more predictive. This could be related to the positive bias of the water levels in the Hollandse IJssel and Lek, shifting the isohalines further downstream. One of the two stations actually has a positive MSS value for storm conditions, showing the modeled peaks during the storm surge are more predictive than the mean of observations. This also holds for the stations at the North Sea, Rotterdam Waterway, and New Meuse.

Figure 4 shows time series between 21 October and 10 November for water level and salinity for one station in each of the six subregions. These stations are indicated in Figure 2. We chose different depths for the stations to show the variability. The last column contains correlation plots of modeled and observed salinity for the whole validation period in light gray and for the selected time series in dark gray. The first three rows are in the tide-dominated region, with a clear tidal signal in both water level and salinity. The model matched the amplitude of the observed tides with no visible phase shift. At Hoek van Holland at −4.5 m NAP, the model slightly overpredicts the salinity during ebb. This is also visible in the correlation plot where the mass of points has a deviation from the 1:1 line toward higher modeled salinities. At Spijkenisse at −9.0 m NAP, the model overpredicts the salinity, whereas higher in the water column (not shown in this plot), the peaks are slightly underestimated. Still, the general trend and peaks are well captured by the model.

For the last three rows, a tidal signal is still visible in water levels but it is not visible anymore (or less visible) in the salinity time series. Same as for the other locations, the tidal signal of modeled water levels matches the observations. The salinity farther upstream is lower and more constant over time. For Zuidland and Krimpen aan de Lek, the model slightly underestimates the observed salinity in October. For the whole year, the correlation plot for Krimpen aan de Lek shows that higher salinities are overestimated by the model. For Zuidland, the relatively rare events with higher salinities match the observations well. Since there are no continuous salinity measurements in the Waal and Meuse, we used an instantaneous measurement for Vuren to check our model. In Appendix A, we show the modeled and observed time series of water level and salinity during the storm period.

3.2. Sinterklaasstorm 5-6 December

In this section, we take a closer look at the storm surge event that occurred on 5–6 December 2013. In the Netherlands, this storm is known as the Sinterklaasstorm, whereas in other literature, it is referred to as storm "Xaver" (e.g., Kettle (2020); Dangendorf et al. (2016)). The locations of the stations mentioned in this section are visualized in Figure 6. The first plot in Figure 5 shows the wind speed at Hoek van Holland. A clear peak is visible on the 5th December exceeding 20 m/s. The second plot shows the corresponding wind vector, which shows the wind direction was west-northwest during the peak (in red).

The water levels in the Rotterdam Waterway (Hoek van Holland) and Haringvliet (Entrance Spui) are almost out of phase (see Figure 5c). The larger-scale northwesterly winds in the North Sea caused set-up at the coast and in the Rotterdam Waterway, which can be seen in Figure 5c. The water levels in the Rotterdam Waterway were 1–1.5 m higher than in the Haringvliet for two tidal cycles. This caused a barotropic flow toward the Haringvliet. The salinity at Hoek van Holland is shown in Figure 5d. While for normal conditions the Rotterdam Waterway is strongly stratified, the water column is well-mixed during the storm when a bulk of salt water enters the Rhine-Meuse Delta. This is also visible from the gradient Richardson number (shown in Figure 5e), with values in the range of the critical Richardson number (0.25–1). A second salinity peak on December 6th is visible at high water. Remarkably, the re-stratification only takes 1–2 days following the storm surge. In the last plot in Figure 5, we see the salt entering the Haringvliet, caused by the reversal of the tide-averaged flow. The peak water level in the Haringvliet is observed 4.5 hr later than at Hoek van Holland, the slow response can be explained by the large storage capacity of the Haringvliet. Due to this and the large water level gradient, a large volume of salt water (approximately 40 million cubic meters) flows into the Haringvliet via the Old Meuse and Spui. To study this in

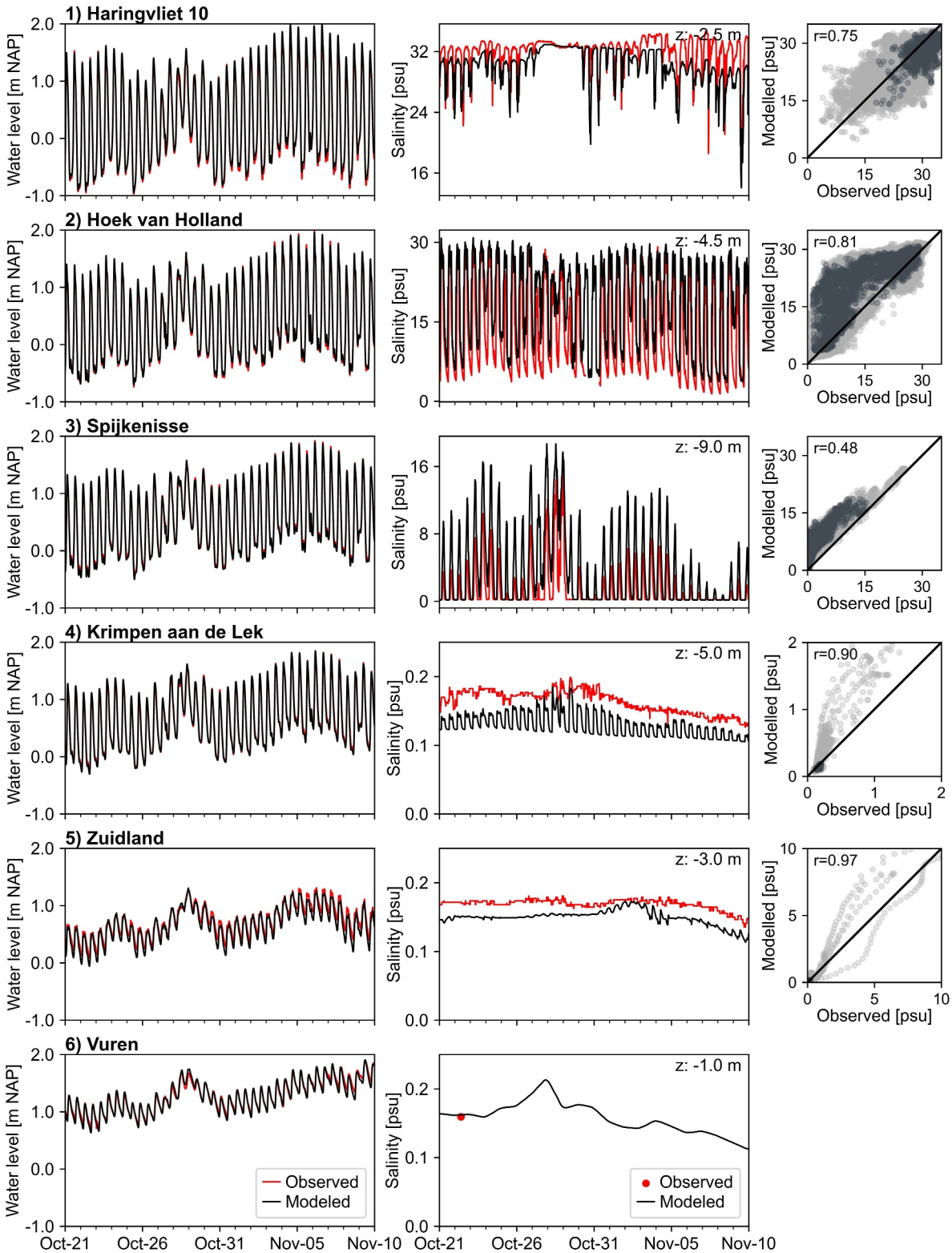

Figure 4. Time series from 21 October to 10 November for water level and salinity for six stations, one station in each of the subregions. Modeled values are in black and observed in red. Last column shows correlation plots between observed and modeled salinity for the whole validation period in light gray and for the selected time series in dark gray. Note the different scales on the *y*-axis for the correlation plots.

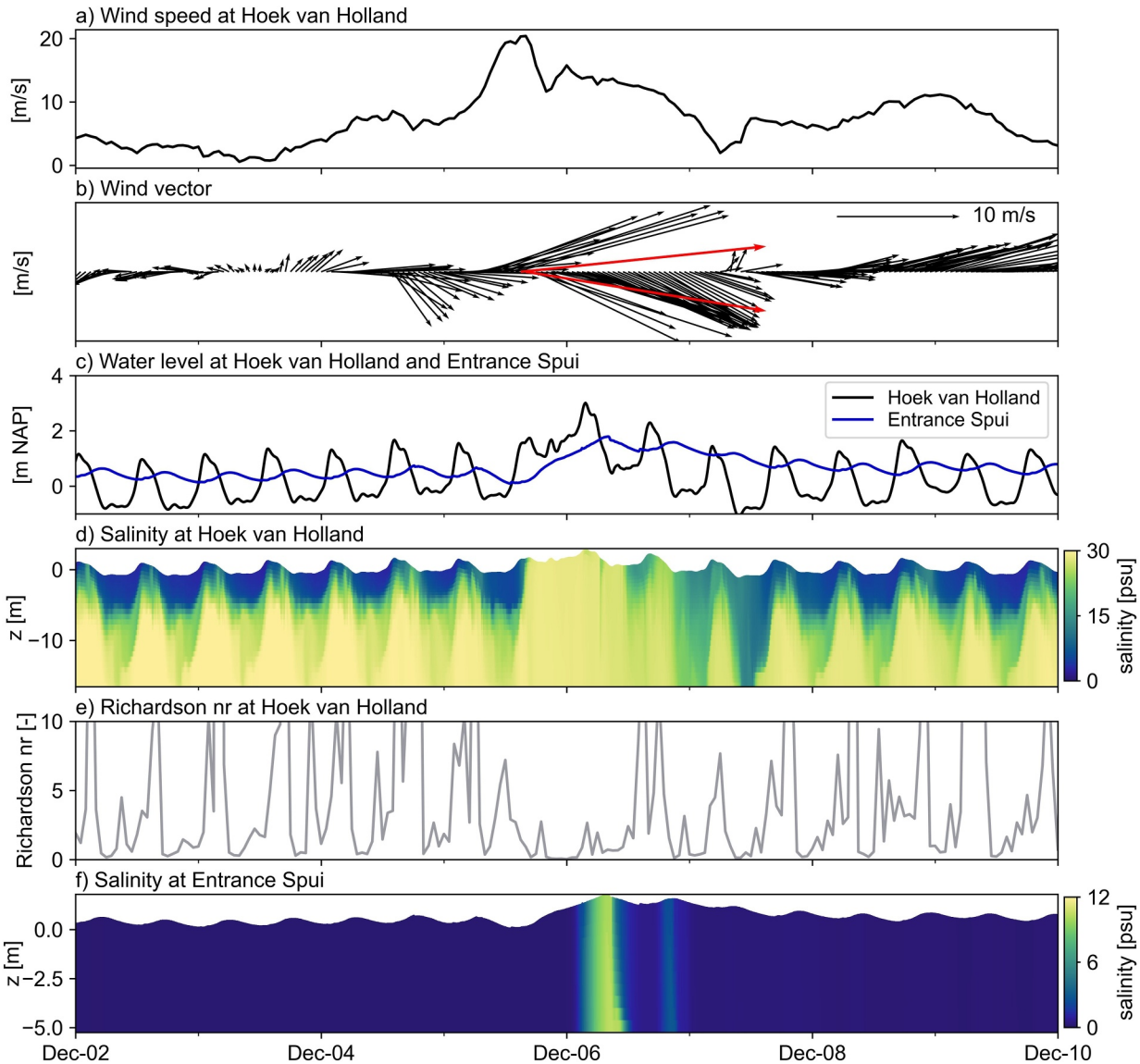

Figure 5. Plot showing wind speed (a), wind vector (b), water level (c), salinity (d), and depth-averaged Richardson number (e) at Hoek van Holland; and water level (c) and salinity (f) at Entrance Spui (at the Haringvliet side) during the 2013 storm period.

more detail, we looked at a cross-section spanning part of the Old Meuse, the Spui channel, and Haringvliet (red line in Figure 6). Figure 6 shows the strong depth variations in the Haringvliet, with deep channels and pits that are remains of the former estuary. We included a deeper channel and pit in the cross-section to illustrate the impact of depth variations on the salt dynamics.

Figure 7 shows the salinity over time in the cross-section, and measured salinity as colored squares in the plots. The simulated salinity matches the observations well for all four locations along the transect. In the first plot, we see the salt going from the Old Meuse into the Spui. The Old Meuse is stratified, whereas the Spui is still well-mixed. Note that the isohalines in the Spui follow the local bathymetry. 4 hr later, the salt reaches the end of the Spui (second plot Figure 7). When the salt water enters the Haringvliet in the third plot, we see the salt creeping over the bottom. In the fourth plot, the salt reaches the lower parts of a deeper channel in the Haringvliet. We also see salt accumulating in the deeper parts at the end of the Spui channel. The salt eventually enters a deep pit (last plots Figure 7). The floodgates in the Haringvlietdam were closed during the storm surge (see Figure 10d) resulting in low flow velocities in the Haringvliet, enhancing stratification. These results show that salt is retained in the deeper parts of the Haringvliet after the storm surge.

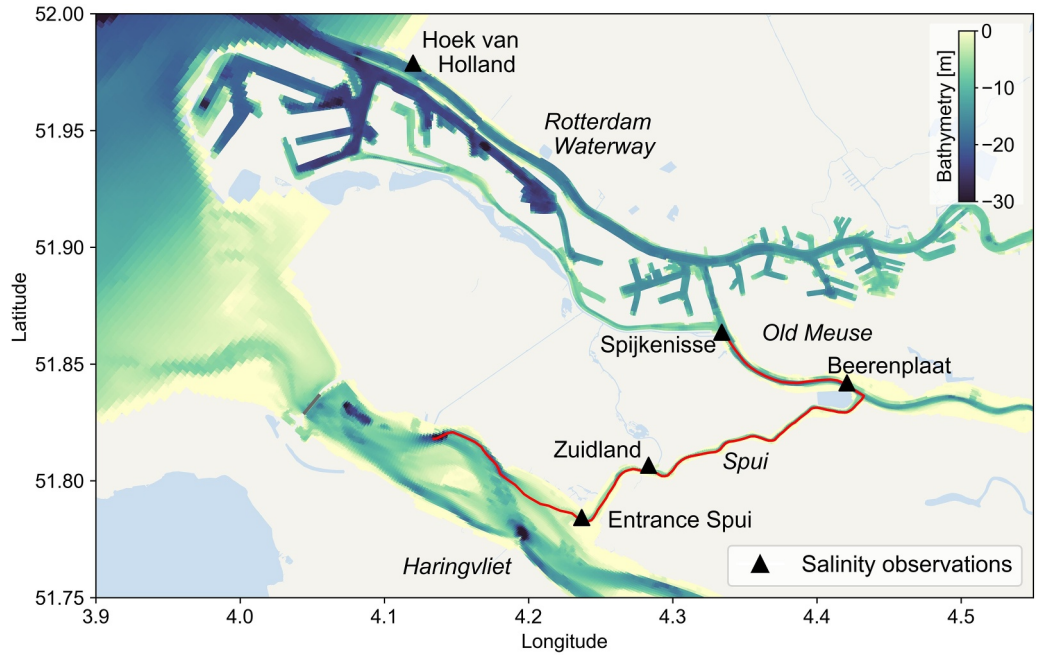

Figure 6. Map showing salinity and water level observations and the cross-section (in red) used for the storm surge analysis. The bathymetry is plotted to show the depths at different parts of the cross-section.

3.3. Post-Storm Horizontal Salt Reflux

In the weeks following the Sinterklaasstorm, salt concentrations exceeding the Dutch norm for freshwater intake were observed in the Spui. The Dutch norm for freshwater intake equals 150 mg/l Chloride, which corresponds to a salinity of 0.27 psu. Figure 8a shows the salinity at Zuidland in the Spui channel. Figure 8b is a close-up of (8a) for the post-storm period. Figure 8c shows the tide-averaged discharge in the Spui channel. A clear peak is visible during the storm (8a), when the flow is directed toward the Haringvliet (8c). A second salinity peak is visible when the flow in the Spui channel is seawards. The peak salinity at Zuidland (40 km from estuarine mouth) is equal to 16 psu, indicating that the peak salinity is about 50 percent seawater (~32 psu).

In the weeks after the storm surge, tide-averaged flow in the Spui channel was seaward (8c) suggesting the higher salinities are caused by a horizontal reflux of salt from the Haringvliet into the Spui channel. Figure 9 shows the salinity in the cross-section (red line Figure 6) on 14 and 15 December. When focusing on the Haringvliet, one can see how the salt in the channel and pit is slowly mixed into the surface layer. Every tidal cycle, salt is slowly released and flows back into the Spui channel. In the last two plots in Figure 9, one can see the salt water flowing from the Haringvliet into the Spui channel. This is consistent with the higher salt concentrations at Zuidland in the weeks after the storm surge (8b). The gray striped line shows the norm for freshwater intake. The observed salinity was close to this norm for 3 weeks and part of the time even above this limit. The model follows the same trend and predicts the higher salinities in the weeks after the storm surge. From this, we can conclude that the 3D model is able to reproduce the horizontal salt reflux.

4. Discussion

Fortunately, not all storms cause backwards salinization like the Sinterklaasstorm in 2013. Figure 10a shows three storms occurred in the last 3 months of 2013, where only one of them, the Sinterklaasstorm on 5-6 December, caused backwards salinization. The water level difference between the Rotterdam Waterway and Haringvliet, visualized in Figure 10c, is the driving factor. Clearly, this difference was largest during the Sinterklaasstorm. Figure 10b shows the water level and astronomical tide at Hoek van Holland, the difference can be seen as a measure for surge. Storm surge is influenced by the air pressure and the wind speed and direction (see Figure 10a). For example, the third storm on 24 December with prevailing northward wind, did not create significant surge. The first storm on 28 October did cause surge; however, the maximum water levels were much higher for the

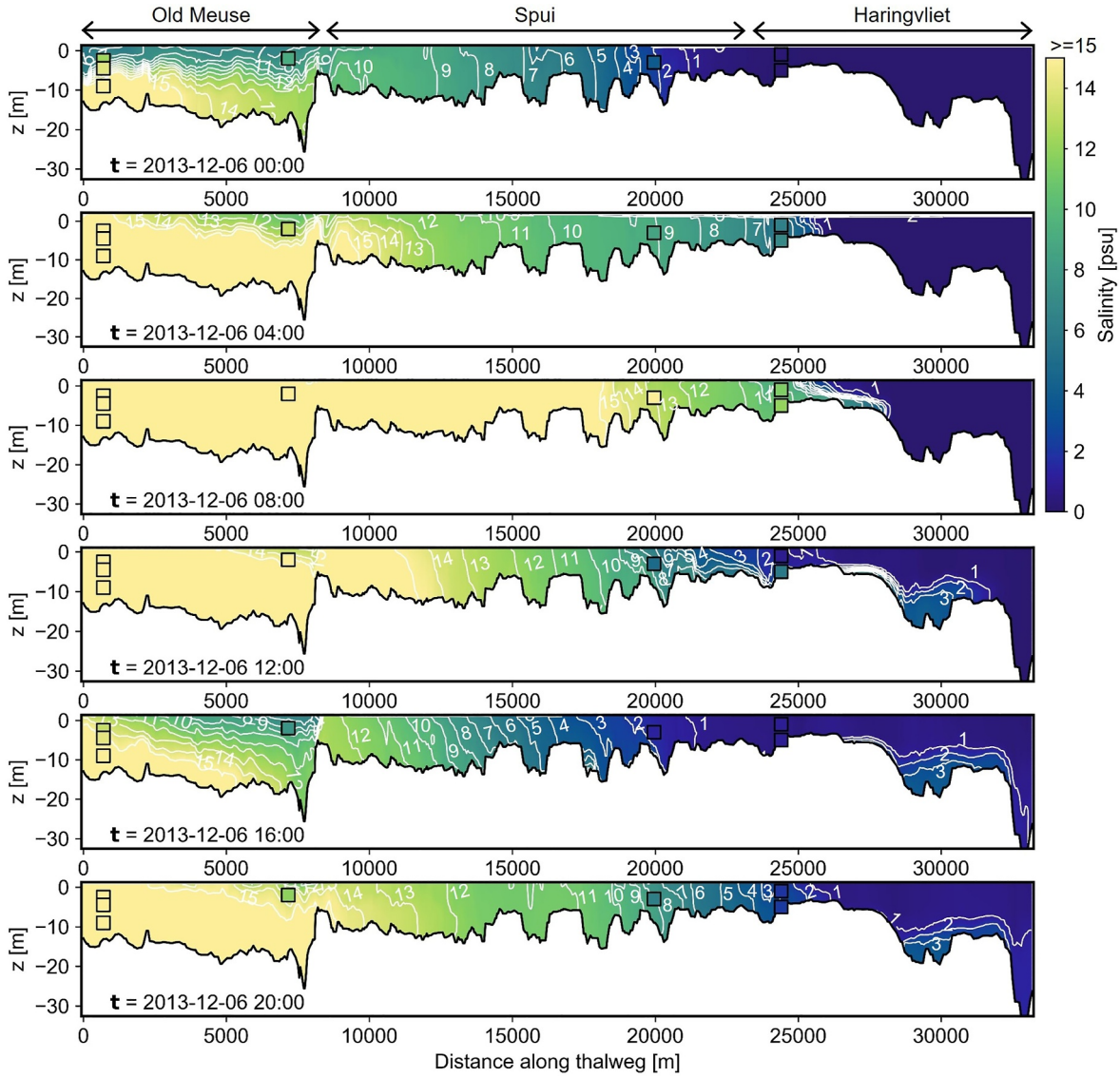

Figure 7. Simulated (contours) and observed (squares) salinity for the cross-section shown in Figure 6 during the storm surge event. The distance along thalweg on the *x*-axis starts at zero in the Old Meuse. The Zuidland station is located at 20,000 m. Parts of the cross-section belonging to the Old Meuse, Spui, and Haringvliet are indicated at the top.

Sinterklaasstorm as it coincided with spring tide. The combination of high surge and spring tide thus caused the high water levels at Hoek van Holland during the Sinterklaasstorm. Furthermore, the water levels in the Haringvliet also affect the gradient, which is strongly affected by the control of the floodgates in the Haringvlietdam. Figure 10d shows the discharge through the floodgates. The day before the Sinterklaasstorm one can see two peak discharges, the floodgates were opened to lower water levels in the domain. This measure lowered the maximum water levels during the storm surge, but likely increased the backwards salinization. This illustrates the complex interaction between human structures and the estuarine response to storm surges. This was also seen for the Yangtze Estuary, where the lower river discharge after the regulation with the Three Gorges Dam contributed to higher salinities after the passing of a tropical cyclone (L. Li et al., 2022).

The closure of the Haringvliet estuary had a big impact on the hydrodynamics. The currents used to be strong in the former estuary, after closure the tidal currents became much weaker and are now controlled by the floodgates in the Haringvlietdam. The Rhine river discharge at Lobith determines whether the gates remain closed $(<1100\ m^3/s)$, partially opened during ebb $(1100 - 1700\ m^3/s)$ or further opened $(>1700\ m^3/s)$. For high

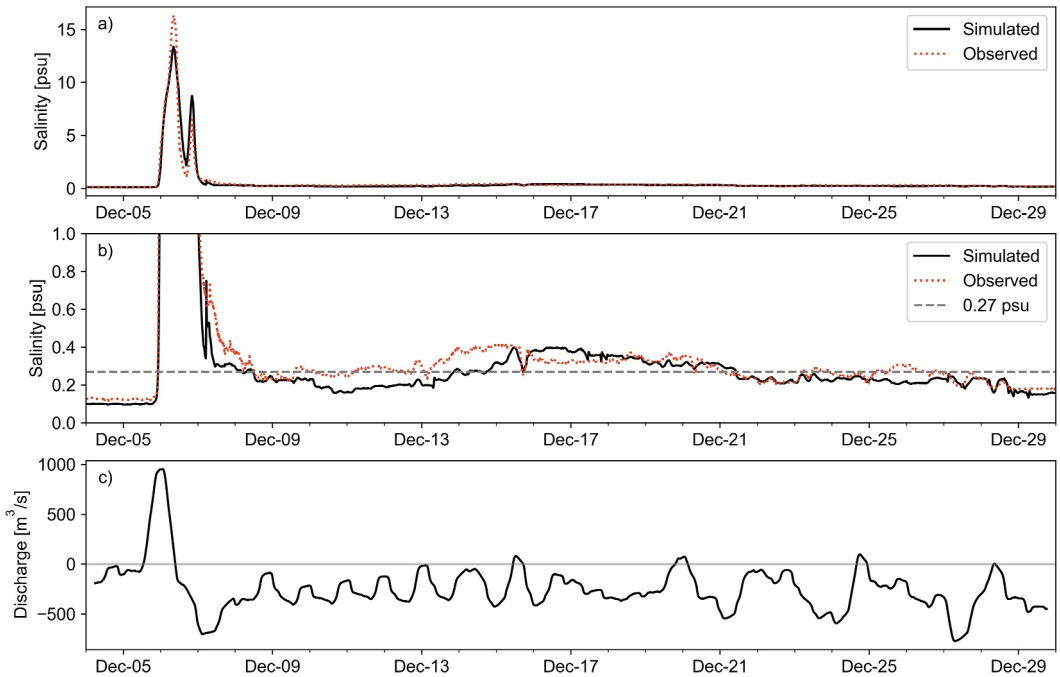

Figure 8. (a) Simulated (black) and observed (red) salinity at Zuidland at 3 m depth. (b) Close-up of (a) for the post-storm period. The gray striped line shows the Dutch norm of 150 mg/L Chloride, equal to 0.27 psu. (c) Tide-averaged discharge in the Spui channel, positive values indicate landward flow and negative values seaward flow.

river discharges, the salt is flushed through the floodgates after the storm. On the other hand, when the floodgates remain closed, flow velocities in the Haringvliet are low, enhancing stratification and long-term retention of salt (Huismans, 2016). Likewise, Chen and Orton (2023) found that river discharge is an important factor governing the impact of gate closure and the recovery time after a storm surge. Figure 10e displays the Rhine discharge at Lobith in the last 3 months of 2013. In the first 2 weeks of December, the Rhine discharge was around 1900 m^3/s, slightly below the average $(2200\ m^3/s)$. A peak discharge through the floodgates is observed after the Sinterklaasstorm (see Figure 10d), yet the flushing was not enough to remove the salt in the deeper parts. This matches the findings of Kranenburg et al. (2023), were they used field observations to study the effects of limited opening the floodgates for fish migration. They found that once the salt reaches the deeper parts of the Haringvliet, above-average discharges were not enough to quickly flush these channels, due to the strong stratification.

Our results show that the salt water has a tendency to move to the deeper parts of the Haringvliet. Yet, the question remains where the salt is exactly after the storm surge. Based on the bathymetry, there are multiple channels and pits where the salt can accumulate. Unfortunately, no field measurements were available for this period to confirm our model results, so this remains uncertain. Nevertheless, our model is able to accurately predict the horizontal salt reflux into the Spui channel. For weeks, the modeled (and measured) salt concentrations were either just below or slightly above the Dutch water quality norm for freshwater intake. Due to the strict norm, small amounts of salt released from the Haringvliet can cause long-lasting problems for fresh water intake. We show how a 3D model can support water managers by giving a more accurate prediction of the duration of the horizontal salt reflux. The salinity at Zuidland is somewhat underpredicted by the model between 10 and 15 December. This corresponds to the period where the water levels in the Haringvliet are underpredicted by the model. The representation of the floodgates in the 3D model is challenging and introduces uncertainties into the predicted water levels. Since the horizontal reflux of salt is partly driven by the water level gradient, reducing the uncertainty in predicted water levels might improve the results.

Previous studies modeled storm surges in 2D and 3D to see the effect on water levels. Zheng et al. (2013) concluded that both 2D and 3D models can predict surge given suitable parameter calibration. However, Ye et al. (2020) found that baroclinic effects can significantly affect water levels in the post-surge adjustment period, requiring a 3D model for accurate water level predictions. The former studies focussed on the baroclinic effects on

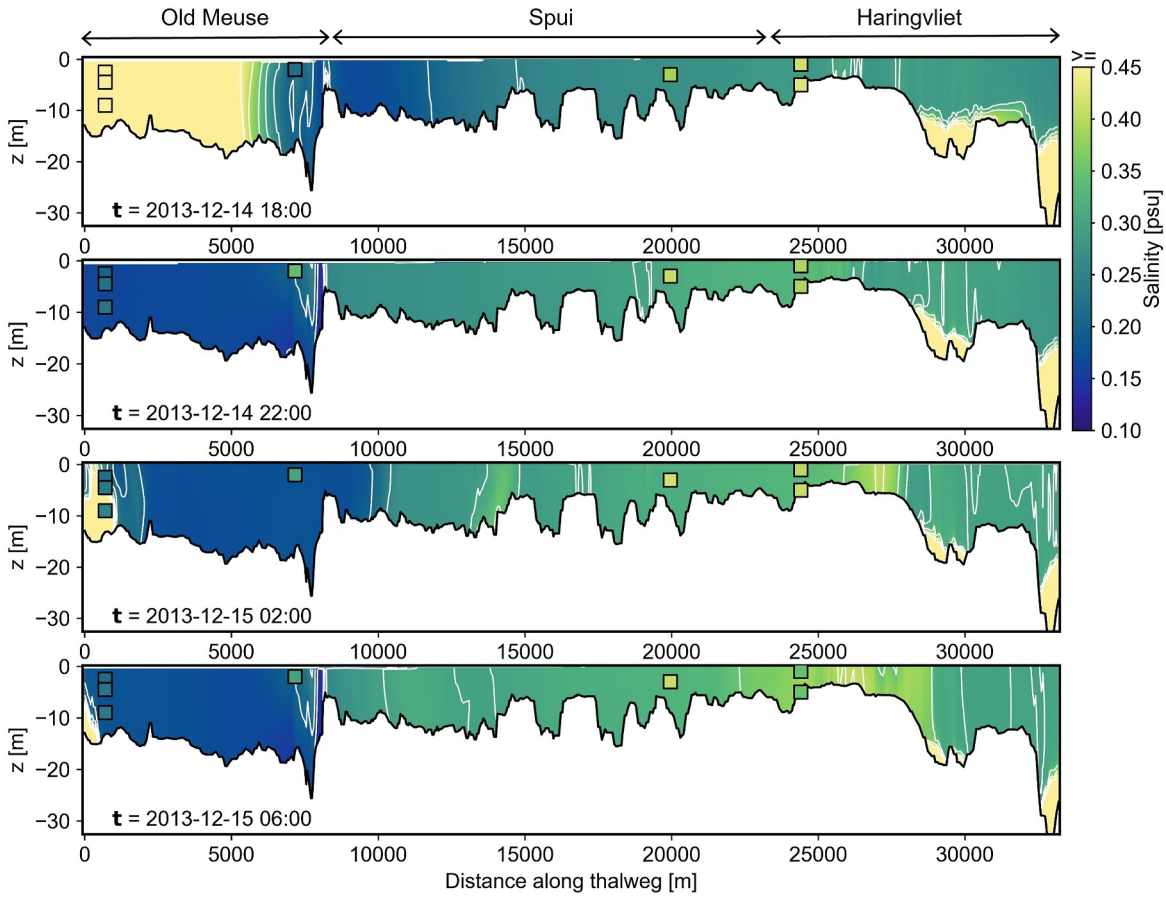

Figure 9. Simulated (contours) and observed (squares) salinity for the cross-section shown in Figure 6 on 14 and 15 December showing the horizontal salt reflux from Haringvliet into the Spui channel.

water levels, not on salinity predictions. As the barotropic flow dominates the salt transport in the Rhine-Meuse Delta during storm surges (Kranenburg et al., 2022), a 2D model likely gives reasonable predictions of salt intrusion during the storm surge. However, our results show that the salt can be retained in regions with relatively weak tidal currents where stratification plays a role, showing the need for a 3D model to forecast salt intrusion during and after a storm surge.

Many estuaries worldwide have been closed off from the sea. For instance, about half of South Korea's estuaries are closed by estuarine dams (Figueroa et al., 2022) and more than 300 of such dams are found along the coast of China (Q. Zhu et al., 2017). While these enclosed regions normally function as freshwater reservoir, they can form a risk for salt intrusion during storm surges. Furthermore, not only an estuarine dam but also a retention area, lake, or dead branch with low flow velocities can store salt after a storm surge. This implies that prolonged salt intrusion after a storm surge could also occur in other deltas. We recommend investigating other deltas where this risk may also be present.

The RMD model captures the physical processes governing salt intrusion during and after storm surges while being able to make predictions on an operational timescale. This could help to optimize water management. For example, to improve the control of the floodgates to minimize salt intrusion. One could test if the backwards salinization after a storm such as the Sinterklaasstorm would have been less when the water levels in the Haringvliet would have been higher before the storm surge. Obviously, there is a trade-off between water safety and water quality, the model could help to find the best solution. Furthermore, the effect of storm surges on salt intrusion can potentially increase with sea level rise and more extreme droughts in a future climate. This further stresses the need for exploring how the floodgates could be put to use for reducing salt intrusion.

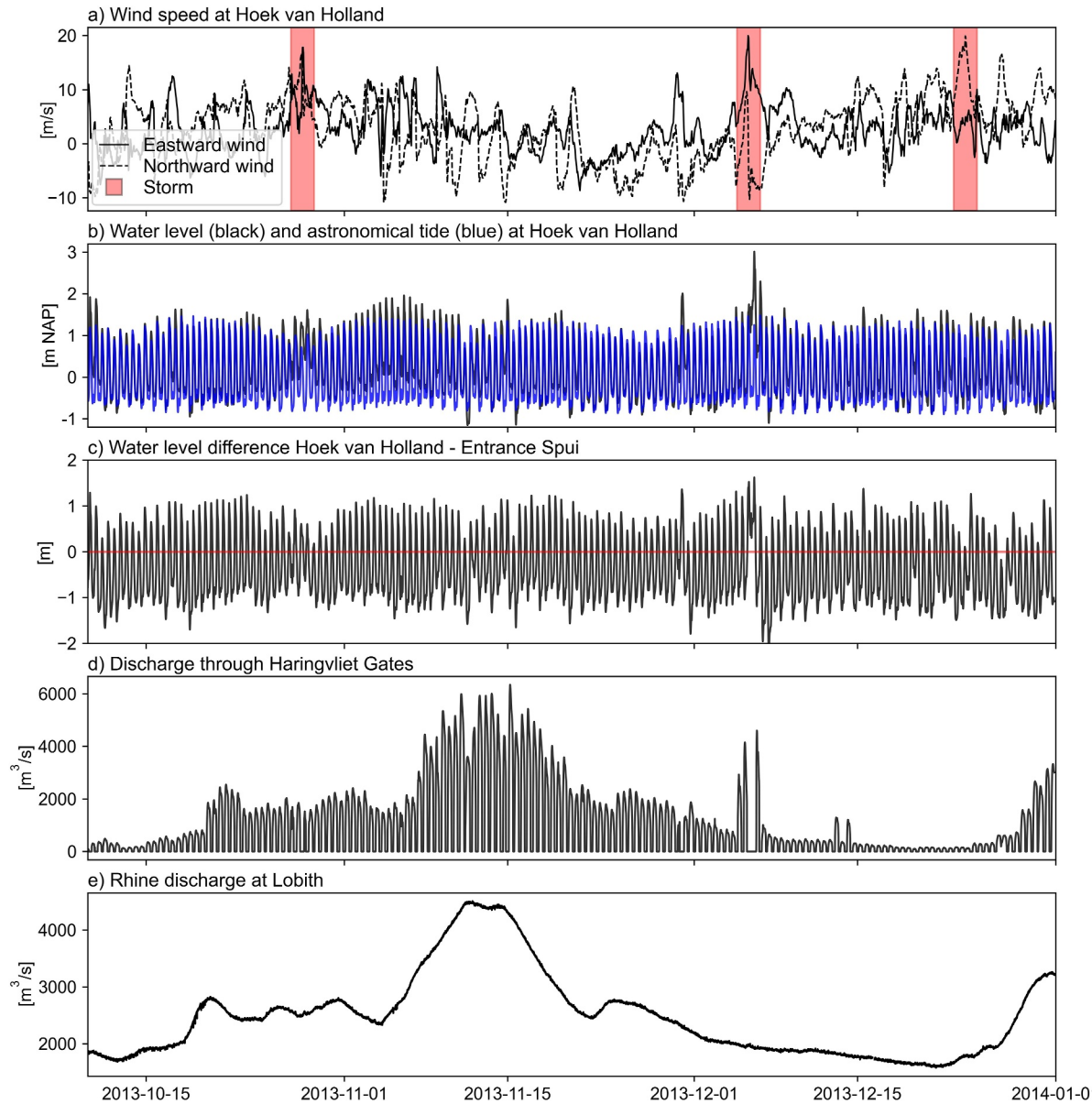

Figure 10. Plots showing (a) Wind speed; (b) Water level and astronomical tide at Hoek van Holland; (c) The water level difference between Hoek van Holland and Entrance Spui; (d) Discharge through the floodgates in the Haringvlietdam; (e) Rhine river discharge at Lobith.

5. Conclusion

In this study, we analyzed the effects of a storm surge event on salt intrusion in the Rhine-Meuse Delta. Most storm surges only temporarily cause increased salt intrusion, yet there have been few cases where elevated salinity levels were observed for weeks. We developed a three-dimensional model of the Rhine-Meuse Delta and simulated an exceptional storm surge event that occurred on 5–6 December 2013. The model validation metrics show that the water level and salinity dynamics are well-captured by the model, both for normal and storm conditions. High water levels in the Rotterdam Waterway due to high surge in combination with spring tide caused landward advection of salt with high salinity peaks throughout the estuary. The water level difference between the northern branch (Rotterdam Waterway) and southern branch (Haringvliet) drove a net salt flux toward the southern branch. The results of the 3D simulation demonstrate three things. First of all, if salt water intrudes into semi-enclosed regions with low flow velocities during a storm surge, it can be retained and cause salt concentrations to be elevated for weeks. While the effects of storm surges on salt intrusion only last for a few days

in general, these results show that the effects can last longer and even outside of drought conditions. Secondly, bathymetry and stratification play an important role, where the salt goes to the deepest parts, limiting the effectiveness of flushing after the storm surge. Lastly, our 3D model uniquely captures the salinity peaks and post-storm horizontal salt reflux, while simultaneously being able to predict on an operational timescale. This opens the door to use 3D models to optimize water management and assess the risks of storm surges on salt intrusion.

Appendix A

Figure A1

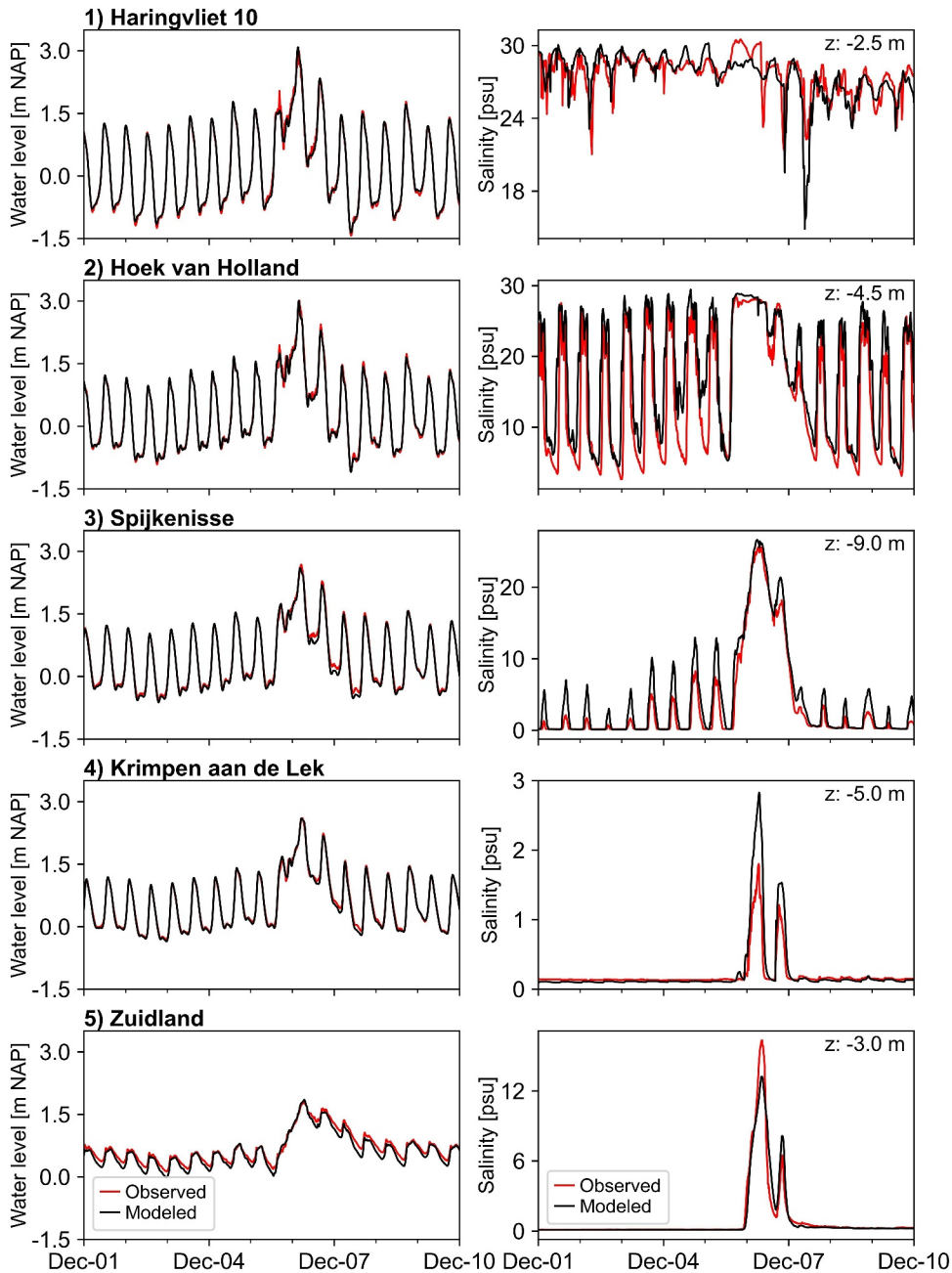

Figure A1. Time series from 1 to 10 December for water level and salinity for Haringvliet 10, Hoek van Holland, Spijkenisse, Krimpen aan de Lek, and Zuidland. Modeled values are in black and observed in red.

Data Availability Statement

The RMD model is developed using the Delft3D-Flexible Mesh (Delft3D-FM) modelling suite by *Deltares* (http://oss.deltares.nl/web/delft3d/home). Model output data used in this study are available at 4TU. ResearchData (https://doi.org/10.4121/ba7df652-cf0d-469a-817c-e783b7b2047c). We used the dfm_tools (https://github.com/Deltares/dfm_tools) for creating the figures and hatyan (https://github.com/Deltares/hatyan) for the harmonic tidal analysis.

Acknowledgments

This study was supported by an NWO Perspective Grant: SALTISolutions (P18-32 Project 9). We would like to show our gratitude to NWO and partners for their support. This work used the Dutch National supercomputer with the support of the SURF Cooperative using Grant EINF-6594. We thank Deltares for providing the software, help, and expertise. We thank Rijkswaterstaat for providing underlying material that was used in the model development, the models that were used to generate boundary conditions (3D DCSM-FM, DCSMv6-ZUNOv4-Kf) and data used for model forcing and validation. Lastly, we thank the anonymous reviewers for their good suggestions that have improved the manuscript.

References

Aristizabal, M. F., & Chant, R. J. (2015). An observational study of salt fluxes in Delaware Bay. *Journal of Geophysical Research: Oceans*, *120*(4), 2751–2768. https://doi.org/10.1038/175238c0

Banas, N. S., Hickey, B. M., MacCready, P., & Newton, J. A. (2004). Dynamics of Willapa Bay, Washington: A highly unsteady, partially mixed estuary. *Journal of Physical Oceanography*, *34*(11), 2413–2427. https://doi.org/10.1175/JPO2637.1

Bowen, M. M., & Geyer, W. R. (2003). Salt transport and the time-dependent salt balance of a partially stratified estuary. *Journal of Geophysical Research*, *108*(C5), 1–15. https://doi.org/10.1029/2001jc001231

Chen, Z., & Orton, P. M. (2023). Effects of storm surge barrier closures on estuary saltwater intrusion and stratification. *Water Resources Research*, *59*(3). https://doi.org/10.1029/2022WR032317

Cho, K. H., Wang, H. V., Shen, J., Valle-Levinson, A., & Cheng Teng, Y. (2012). A modeling study on the response of Chesapeake Bay to hurricane events of Floyd and Isabel. *Ocean Modelling*, *49–50*, 22–46. https://doi.org/10.1016/j.ocemod.2012.02.005

Cook, S. E., Warner, J. C., & Russell, K. L. (2023). A numerical investigation of the mechanisms controlling salt intrusion in the Delaware Bay estuary. *Estuarine, Coastal and Shelf Science*, *283*, 108257. https://doi.org/10.1016/j.ecss.2023.108257

Cox, J. R., Huismans, Y., Knaake, S. M., Leuven, J. R., Vellinga, N. E., van der Vegt, M., et al. (2021). Anthropogenic effects on the contemporary sediment budget of the lower rhine-Meuse delta channel network. *Earth's Future*, *9*(7), 1–22. https://doi.org/10.1029/2020EF001869

Dangendorf, S., Arns, A., Pinto, J. G., Ludwig, P., & Jensen, J. (2016). The exceptional influence of storm "Xaver" on design water levels in the German Bight. *Environmental Research Letters*, *11*(5), 054001. https://doi.org/10.1088/1748-9326/11/5/054001

de Nijs, M. A., Pietrzak, J. D., & Winterwerp, J. C. (2011). Advection of the salt wedge and evolution of the internal flow structure in the rotterdam waterway. *Journal of Physical Oceanography*, *41*(1), 3–27. https://doi.org/10.1175/2010JPO4228.1

De Vries, I. (2014). *Toetsing robuustheid Brielse meer voor zoetwatervoorziening* (Technical Report No. 1209018-000-VEB-0004). Deltares.

Eslami, S., Hoekstra, P., Kernkamp, H. W., Nguyen Trung, N., Do Duc, D., Nguyen Nghia, H., et al. (2021). Dynamics of salt intrusion in the Mekong Delta: Results of field observations and integrated coastal-inland modelling. *Earth Surface Dynamics*, *9*(4), 953–976. https://doi.org/10.5194/esurf-9-953-2021

Figueroa, S. M., hong Lee, G., Chang, J., & Jung, N. W. (2022). Impact of estuarine dams on the estuarine parameter space and sediment flux decomposition: Idealized numerical modeling study. *Journal of Geophysical Research: Oceans*, *127*(5). https://doi.org/10.1029/2021JC017829

Fischer, H. (1972). Mass transport mechanisms in partially stratified estuaries. *Journal of Fluid Mechanics*, *53*(4), 671–687. https://doi.org/10.1017/s0022112072000412

Flather, R. A. (2001). Storm surges. In *Encyclopedia of ocean sciences* (pp. 2882–2892). https://doi.org/10.1006/rwos.2001.0124

Hansen, D. V., & Rattray, M. (1965). Gravitational circulation in straits and estuaries. *Journal of Marine Research*, *23*, 104–122.

Hu, K., Meselhe, E. A., & Reed, D. J. (2023). Understanding drivers of salinity and temperature dynamics in Barataria estuary, Louisiana. *Journal of Geophysical Research: Oceans*, *128*(7), 1–19. https://doi.org/10.1029/2023JC019635

Huismans, Y. (2016). *Systeemanalyse Rijn- Maasmonding: Analyse relaties noord- En Zuidrand En Gevoeligheid stuurknoppen* (Technical Report No. 1230077-001-ZWS-001 0). Deltares.

Huismans, Y., Groenenboom, J., Zijl, F., & van der Wijk, R. (2019). *Voorspellen optreden nalevering bij Bernisse* (Technical Report No. 11203734-008-ZWS-0003). Deltares.

Kernkamp, H. W., Van Dam, A., Stelling, G. S., & De Goede, E. D. (2011). Efficient scheme for the shallow water equations on unstructured grids with application to the Continental Shelf. *Ocean Dynamics*, *61*(8), 1175–1188. https://doi.org/10.1007/s10236-011-0423-6

Kettle, A. J. (2020). Storm Xaver over Europe in December 2013: Overview of energy impacts and North Sea events. *Advances in Geosciences*, *54*(December 2013), 137–147. https://doi.org/10.5194/adgeo-54-137-2020

Kranenburg, W., Tiessen, M., Blaas, M., & Van Veen, N. (2023). Circulation, stratification and salt dispersion in a former estuary after reintroducing seawater inflow. *Estuarine, Coastal and Shelf Science*, *282*, 108221. https://doi.org/10.1016/j.ecss.2023.108221

Kranenburg, W., Van der Kaaij, T., Tiessen, M., Friocourt, Y., & Blaas, M. (2022). Salt intrusion in the Rhine-Meuse delta: Estuarine circulation, tidal dispersion or surge effect? In *Iahr world congress* (pp. 5601–5608).

Lerczak, J. A., Geyer, W. R., & Chant, R. J. (2006). Mechanisms driving the time-dependent salt flux in a partially stratified estuary. *Journal of Physical Oceanography*, *36*(12), 2296–2311. https://doi.org/10.1175/JPO2959.1

Lerczak, J. A., Geyer, W. R., & Ralston, D. K. (2009). The temporal response of the length of a partially stratified estuary to changes in river flow and tidal amplitude. *Journal of Physical Oceanography*, *39*(4), 915–933. https://doi.org/10.1175/2008JPO3933.1

Li, L., Wang, C., Pareja-Roman, L. F., Zhu, J., Chant, R. J., & Wang, G. (2022). Effects of Typhoon on saltwater intrusion in a high discharge estuary. *Journal of Geophysical Research: Oceans*, *127*(8), 1–17. https://doi.org/10.1029/2021JC018206

Li, M., Zhong, L., & Boicourt, W. C. (2005). Simulations of Chesapeake Bay estuary: Sensitivity to turbulence mixing parameterizations and comparison with observations. *Journal of Geophysical Research*, *110*(12), 1–22. https://doi.org/10.1029/2004JC002585

Orton, P., Ralston, D., van Prooijen, B., Secor, D., Ganju, N., Chen, Z., et al. (2023). Increased utilization of storm surge barriers: A research agenda on estuary impacts. *Earth's Future*, *11*(3). https://doi.org/10.1029/2022EF002991

Ralston, D. K. (2022). Impacts of storm surge barriers on Drag, mixing, and exchange flow in a partially mixed estuary Journal of Geophysical research: Oceans. *Journal of Geophysical Research: Oceans*, *127*(4), 1–21. https://doi.org/10.1029/2021JC018246

Ralston, D. K., Geyer, W. R., & Lerczak, J. A. (2010). Structure, variability, and salt flux in a strongly forced salt wedge estuary. *Journal of Geophysical Research*, *115*(6), 1–21. https://doi.org/10.1029/2009JC005806

Tönis, I., Stam, J., & Van de Graaf, J. (2002). Morphological changes of the Haringvliet estuary after closure in 1970. *Coastal Engineering*, *44*(3), 191–203. https://doi.org/10.1016/s0378-3839(01)00026-6

Tsai, C. S., Hoque, M. A., Vineis, P., Ahmed, K. M., & Butler, A. P. (2024). Salinisation of drinking water ponds and groundwater in coastal Bangladesh linked to tropical cyclones. *Scientific Reports*, *14*(5211), 5211. https://doi.org/10.1038/s41598-024-54446-6

van der Kaaij, T., & Chavarrias, V. (2020). *D-HYDRO RijnMaasMonding 3D; Zoutindringing in de Nieuwe Waterweg* (Technical Report No. 11205258-016-ZWS-0003). Deltares.

van Rijn, L. C. (1984). Sediment transport, Part III: Bed form and alluvial roughness. *Journal of Hydraulic Engineering*, *110*(2), 1733–1754.

Ye, F., Zhang, Y. J., Yu, H., Sun, W., Moghimi, S., Myers, E., et al. (2020). Simulating storm surge and compound flooding events with a creek-to-ocean model: Importance of baroclinic effects. *Ocean Modelling*, *145*, 101526. https://doi.org/10.1016/j.ocemod.2019.101526

Zheng, L., Weisberg, R. H., Huang, Y., Luettich, R. A., Westerink, J. J., Kerr, P. C., et al. (2013). Implications from the comparisons between two- and three-dimensional model simulations of the Hurricane Ike storm surge. *Journal of Geophysical Research: Oceans*, *118*(7), 3350–3369. https://doi.org/10.1002/jgrc.20248

Zhu, J., Cheng, X., Li, L., Wu, H., Gu, J., & Lyu, H. (2020). Dynamic mechanism of an extremely severe saltwater intrusion in the Changjiang estuary in February 2014. *Hydrology and Earth System Sciences*, *24*(10), 5043–5056. https://doi.org/10.5194/hess-24-5043-2020

Zhu, Q., Wang, Y. P., Gao, S., Zhang, J., Li, M., Yang, Y., & Gao, J. (2017). Modeling morphological change in anthropogenically controlled estuaries. *Anthropocene*, *17*, 70–83. https://doi.org/10.1016/j.ancene.2017.03.001

Zijl, F., Sumihar, J., & Verlaan, M. (2015). Application of data assimilation for improved operational water level forecasting on the northwest European shelf and North Sea. *Ocean Dynamics*, *65*(12), 1699–1716. https://doi.org/10.1007/s10236-015-0898-7